

HgTe-CdTe superlattices for infrared detection revisited

T. H. Myers

Department of Physics, West Virginia University, Morgantown, West Virginia 26506

J. R. Meyer and C. A. Hoffman

Naval Research Laboratory, Washington, DC 20375

L. R. Ram-Mohan

Worcester Polytechnic Institute, Worcester, Massachusetts 01609

(Received 6 April 1992; accepted for publication 11 August 1992)

Selected properties of HgTe-CdTe superlattices are re-examined in light of the new consensus that the valence-band offset is large. We conclude that while the cutoff wavelength for infrared detectors remains easier to control in superlattices than in the corresponding $\text{Hg}_{1-x}\text{Cd}_x\text{Te}$ alloy, the advantage is less than was predicted earlier assuming a small offset. The reduction of tunneling noise and minority carrier collection efficiency are discussed on the basis of revised electron and hole masses in the growth direction.

In 1979, HgTe-CdTe superlattices (SLs) were first proposed as promising new infrared materials with properties quite distinct from those of $\text{Hg}_{1-x}\text{Cd}_x\text{Te}$ alloys.¹ Several groups subsequently pointed out that this SL system should present significant advantages for long wavelength infrared (LWIR) and very long wavelength infrared (VLWIR) detectors.²⁻⁴ Of practical interest was the prediction that the band gap of the SL could be much easier to control than that of the alloy. It was also argued that since growth-direction effective masses in the SL are decoupled from the band gap, LWIR detectors with larger masses would display orders of magnitude reductions in the tunneling current. However, those analyses were performed at a time when the understanding of the HgTe-CdTe system was still largely incomplete. In particular, all of the studies cited above were based on the assumption of a small valence-band offset, $\Delta E_V < 40$ meV. It is now recognized that numerous aspects of the SL properties can only be understood in terms of a large ΔE_V ,⁵ the most frequently employed value being 350 meV.⁶ The recent fabrication by molecular beam epitaxy (MBE) of a high quantum efficiency SL detector operating at $5\ \mu\text{m}$ ⁷ makes it particularly worthwhile to reassess the earlier predictions of SL detector properties. In this letter we will analyze ramifications of the larger valence-band offset for such performance considerations as cutoff wavelength control, tunneling currents, and photogenerated charge collection efficiency.

The calculations presented in this letter were performed using an eight-band $k \cdot p$ formalism^{8,9} including the effects of strain, with $\Delta E_V = 350$ meV. The barrier layers were taken to be $\text{Hg}_{0.15}\text{Cd}_{0.85}\text{Te}$ for [100] growth and $\text{Hg}_{0.10}\text{Cd}_{0.90}\text{Te}$ for [211] growth rather than pure CdTe.

For a typical detector operating temperature of 77 K, Fig. 1 shows calculated SL cutoff wavelengths ($\lambda_C \equiv 2\pi\hbar c/E_g$) as a function of HgTe well thickness, d_W . The barrier thickness (d_B) is held constant at 50 Å, and results for both the [100] (dashed) and [211] (solid) orientations are given. Also shown for comparison are the early results of Smith *et al.* ($d_B = d_W$),² who assumed a valence-band offset of zero. It is evident that this and other earlier estimates of

the appropriate well thicknesses for LWIR detectors must be revised considerably.

At some finite composition x , the band gap in the $\text{Hg}_{1-x}\text{Cd}_x\text{Te}$ alloy goes to zero, leading to a singularity in the cutoff wavelength. Therefore, to adequately control λ_C for longer wavelengths, one must control the composition to progressively higher precision. Based on calculations employing a small valence-band offset, it has been argued that the SL potentially offers better control of the cutoff wavelength.²⁻⁴ This is because λ_C is then a more slowly varying function of layer thickness, as indicated by the dotted curve in Fig. 1. However, the solid and dashed curves show that with $\Delta E_V = 350$ meV, E_g in the SL goes to zero much faster than was previously believed, as result which has been confirmed experimentally.⁹ Using the calculated $\lambda_C(d_W)$ from Fig. 1, Fig. 2 plots the derivative of $\lambda_C(d_W)$ for the [211] and [100] orientations, along with the prior result for a vanishing valence-band offset. The figure shows that the sensitivity of λ_C to d_W is approximately 2-4 times greater than had previously been believed.

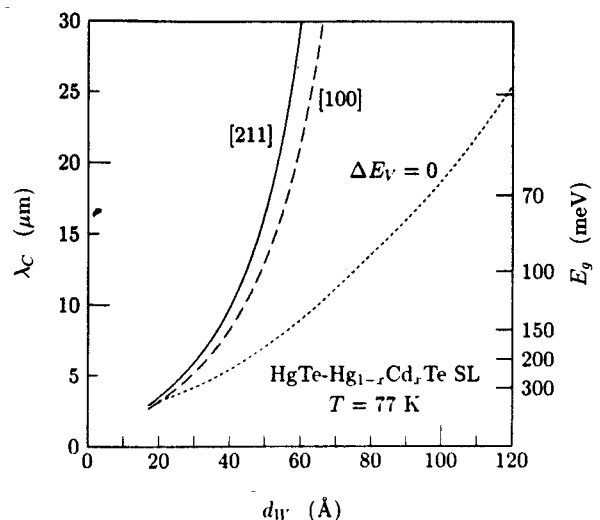


FIG. 1. Cutoff wavelength and energy gap vs well thickness for [100] (dashed curve) and [211] (solid curve) superlattices with $d_B = 50$ Å at 77 K. The dotted curve ($d_B = d_W$) represents the early calculation of Smith *et al.* (Ref. 2), which assumed a valence-band offset of zero.

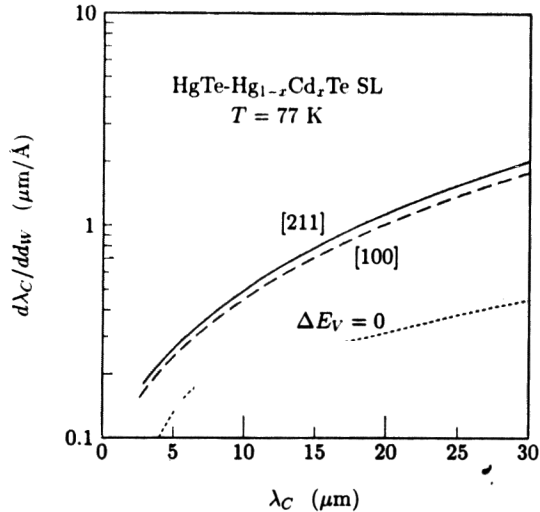


FIG. 2. Derivatives of $\lambda_C(d_w)$ vs cutoff wavelength, from the curves in Fig. 1.

We will follow the procedure outlined by Reno *et al.*⁴ to examine the consequences of the dispersion of λ_C with layer thickness. From reflection high energy electron diffraction (RHEED) oscillations,^{10,11} average HgTe and CdTe growth rates can, in general, be determined to a higher degree of accuracy than fluctuations which occur during growth. The main uncertainty in the control of cutoff wavelength then results from variations in flux from the MBE furnaces, which in turn are due primarily to fluctuations in the MBE source temperatures. The temperature control of MBE furnace typically leads to fluctuations ΔT of order 0.1 °C. For this ΔT , the variation in flux ΔF from an effusion cell can be calculated theoretically¹² using published vapor pressure data. However, since experimental results tend to exceed the calculated values by about a factor of 2 in regions where the comparison can be made,⁴ we have doubled the theoretical flux variations in the following analysis. This yields $\Delta F_{\text{Te}}/F_{\text{Te}} \cong 0.006$ and $\Delta F_{\text{CdTe}}/F_{\text{CdTe}} \cong 0.003$. Assuming ΔT for each effusion cell to be independent of the other cells, the composition fluctuation for the alloy is given by⁴

$$\Delta x = x(1-x) [(\Delta F_{\text{Te}}/F_{\text{Te}})^2 + (\Delta F_{\text{CdTe}}/F_{\text{CdTe}})^2]^{1/2}. \quad (1)$$

Employing the empirical expression of Hansen *et al.*¹³ for $E_g(x)$, we obtain the solid curve in Fig. 3 for the cutoff wavelength fluctuation $\Delta\lambda$ as a function of cutoff wavelength in the alloy.

Since λ_C in the SL depends relatively weakly on the CdTe barrier thickness, $\Delta\lambda$ is due primarily to fluctuations in the HgTe well thickness: $\Delta d_w \approx d_w(\Delta F_{\text{Te}}/F_{\text{Te}})$. Using the values of $d\lambda_C/dd_w$ from Fig. 2, Fig. 3 gives $\Delta\lambda$ for both 0 (dotted curve) and 350 meV [dashed curve, (211) only] valence-band offsets. We find that the cutoff wavelength is still more easily controlled in the SL than in the alloy, although the improvement is smaller than originally predicted using $\Delta E_V = 0$.

Besides reducing the fluctuations in cutoff wavelength, HgTe-CdTe SLs are attractive for IR detectors because one

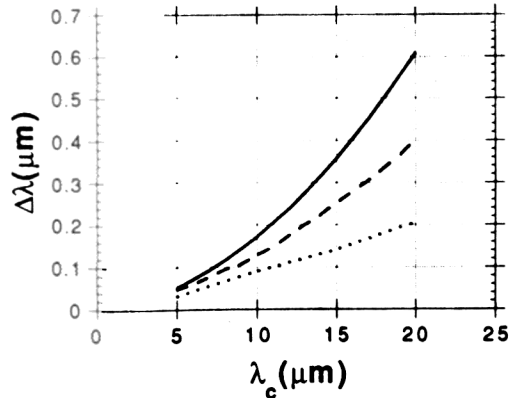


FIG. 3. Calculated cutoff wavelength fluctuations vs cutoff wavelength, due to variations in the MBE effusion cell temperatures. Results are shown for the $\text{Hg}_{1-x}\text{Cd}_x\text{Te}$ alloy (solid curve), and for HgTe-CdTe SLs with valence-band offsets of 0 (dotted curve) and 350 meV (dashed curve).

can tailor the electron and hole transport and tunneling in the growth direction through varying d_B . Our analysis of this topic must, at present, rely primarily on inferences drawn from the calculated electron and hole effective masses along the growth axis (m_z). Published measurements^{14,15} of growth-direction transport have dealt primarily with *resonant* tunneling through single and double heterostructures, and thus have marginal direct relevance to IR detector design and operation.

The magnitude of the valence-band offset affects both m_{nz} and m_{pz} although the hole mass is far more sensitive because ΔE_V determines the ordering of the LH1 and HH1 bands.⁵ For a small offset, strain causes LH1 to be highest in energy and one obtains $m_{pz} \approx m_{nz}$. However, when ΔE_V is large, quantum confinement moves LH1 to an energy well below HH1 and $m_{pz} \gg m_{nz}$. This is illustrated in Fig. 4, which gives theoretical electron and hole masses in the growth direction as a function of barrier thickness for $\Delta E_V = 350$ meV (d_w is varied with d_B , such that E_g remains fixed at 83 meV). Also shown are experimental electron masses for two [211] SLs with $E_g \approx 90$ meV (filled points)^{9,16} and two [100] SLs with $E_g \approx 30$ meV (open points).^{17,18} The agreement between calculated and measured m_{nz} in those regions where the comparison can be made confirms the reliability of the theory.

The figure shows that both m_{nz} and m_{pz} can be tuned over a considerable range by varying d_B . As had been predicted by the early zero-offset calculations, m_{nz} considerably exceeds the electron mass in the alloy with the same band gap ($0.0065m_0$ for $E_g = 83$ meV). Kinch and Goodwin³ (see also Smith *et al.*²) have pointed out that this should lower the tunneling currents by up to several orders of magnitude in photovoltaic LWIR and VLWIR devices fabricated from HgTe-CdTe SLs.

In photovoltaic SL detectors, the growth-direction electron and hole masses also determine to a large extent the photogenerated charge collection efficiency, which depends on the minority carrier diffusion length: $\Lambda \propto (\mu_z \tau_R)^{1/2}$. Here, μ_z is the mobility along the growth axis and τ_R is the recombination lifetime. Note that for any

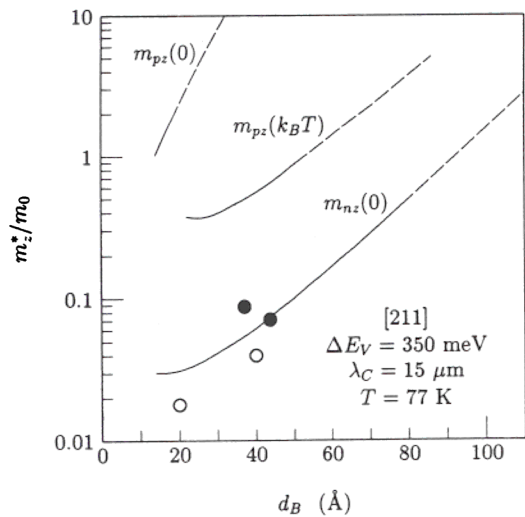


FIG. 4. Theoretical (curves) and experimental (points) growth-direction electron and hole effective masses vs barrier thickness, for [211] superlattices at $T=77$ K. In the theory, the well thickness is varied with d_B such that the energy gap remains constant at 83 meV. Hole masses are given for both the top of the valence band ($E=0$) and for an energy $k_B T$ farther down. The curves are dashed in regions where one expects hopping transport rather than miniband conduction. The electron cyclotron resonance data are from two [211] superlattices with $E_g \approx 30$ meV (open points, Refs. 17 and 18).

$d_B > 20$ Å, holes at the valence-band maximum [$m_{pz}(0)$] have an extremely large mass, implying that they are essentially localized in the low-temperature limit. However, the valence band in HgTe-CdTe SLs displays a “mass-broadening” effect,⁵ which causes the in-plane mass to depend strongly on growth-direction wave vector and m_z to depend strongly on energy. Figure 4 indicates that $m_{pz}(k_B T)$ is orders of magnitude smaller than $m_{pz}(0)$, having a value comparable to the heavy hole mass in the $\text{Hg}_{1-x}\text{Cd}_x\text{Te}$ alloy. This implies that the mobility μ_{pz} may be large enough to allow high collection efficiency as long as d_B is not too thick. However, a further complication is that one expects the miniband conduction model to break down above some critical barrier thickness. The miniband approach is only appropriate when the tunneling time $\tau_T \approx \hbar/W$ (W is the miniband width) is shorter than the scattering time τ_s . When $\tau_T > \tau_s$, the basis states are confined to a single quantum well with only occasional tunneling to an adjacent well. “Growth-direction mass” then becomes an invalid concept, and the transport is primarily by hopping from one well to the next. Since hopping mobilities tend to be far lower than miniband mobilities,¹⁹ one expects poor collection efficiencies at any d_B for which the minority carrier transport must depend on that mechanism. In Fig. 4, the miniband and hopping regimes are indicated by the solid and dashed portions of the curves, respectively, where we have estimated τ_s from the experimental magnetotransport and magneto-optical data.^{5,9} In-

hibited hole transport in the n -doped collection region may explain the reduction at low temperatures of the high quantum efficiency observed for the only published HgTe-CdTe SL mid-wave IR (MWIR) photovoltaic detector (with $d_B = 50$ Å).⁷

In summary, we have re-examined the fundamental reasons behind the interest in HgTe-CdTe SLs as IR detector materials. We conclude that the basic premises reached by earlier workers using $\Delta E_V \approx 0$ remain valid when a large offset is employed. The cutoff wavelength is still easier to control in the SL vs the alloy, and the electron effective mass in the growth direction is large enough to limit tunneling currents. In addition, we have used calculated electron and hole dispersion relations in the growth direction to study qualitative aspects of the transport along that axis. Since LWIR superlattices with lifetimes comparable to those in alloys with the same energy gap have already been achieved,^{16,20} LWIR and VLWIR HgTe-CdTe detectors with high quantum efficiency seem quite feasible and attractive.

The authors would like to acknowledge useful conversations with Dr. N. C. Giles. Work at NRL was supported in part by the Office of Naval Research.

- ¹J. N. Schulman and T. C. McGill, *Appl. Phys. Lett.* **34**, 663 (1979).
- ²D. L. Smith, T. C. McGill, and J. N. Schulman, *Appl. Phys. Lett.* **43**, 180 (1983).
- ³M. A. Kinch and M. W. Goodwin, *J. Appl. Phys.* **58**, 4455 (1985).
- ⁴J. Reno and J. P. Faurie, *Appl. Phys. Lett.* **49**, 409 (1986).
- ⁵J. R. Meyer, C. A. Hoffman, F. J. Bartoli, J. W. Han, J. W. Cook, Jr., J. F. Schetzina, X. Chu, J. P. Faurie, and J. N. Schulman, *Phys. Rev. B* **38**, 2204 (1988).
- ⁶S. P. Kowalczyk, J. T. Cheung, E. A. Kraut, and R. W. Grant, *Phys. Rev. Lett.* **56**, 1605 (1986).
- ⁷K. A. Harris, T. H. Myers, R. W. Yanka, L. M. Mohnkern, and N. Otsuka, *J. Vac. Sci. Technol. B* **9**, 1752 (1991).
- ⁸L. R. Ram-Mohan, K. H. Yoo, and R. L. Aggarwal, *Phys. Rev. B* **38**, 6151 (1988).
- ⁹C. A. Hoffman, J. R. Meyer, R. J. Wagner, F. J. Bartoli, X. Chu, J. P. Faurie, L. R. Ram-Mohan, and H. Xie, *J. Vac. Sci. Technol. A* **8**, 1200 (1990).
- ¹⁰J. Arias and J. Singh, *Appl. Phys. Lett.* **55**, 1561 (1989).
- ¹¹I. Ulmer, N. Magnea, H. Maitte, and P. Gentile, *J. Cryst. Growth* **111**, 711 (1991).
- ¹²D. L. Smith and V. Y. Pickhardt, *J. Appl. Phys.* **46**, 2366 (1975).
- ¹³G. L. Hansen, J. L. Schmit, and T. N. Casselman, *J. Appl. Phys.* **53**, 7099 (1982).
- ¹⁴M. A. Reed, R. J. Koestner, M. W. Goodwin, and H. F. Schaake, *J. Vac. Sci. Technol. A* **6**, 2619 (1988).
- ¹⁵D. H. Chow, T. C. McGill, I. K. Sou, J. P. Faurie, and C. W. Nieh, *Appl. Phys. Lett.* **52**, 54 (1988).
- ¹⁶K. A. Harris, R. W. Yanka, L. M. Mohnkern, T. H. Myers, Z. Yang, Z. Yu, S. Hwang, and J. F. Schetzina, *J. Vac. Sci. Technol. B* (in press).
- ¹⁷M. Dobrowolska, T. Wojtowicz, H. Luo, J. K. Furdyna, O. K. Wu, J. N. Schulman, J. R. Meyer, C. A. Hoffman, and F. J. Bartoli, *Phys. Rev. B* **41**, 5084 (1990).
- ¹⁸J. Manasses, Y. Guldner, J. P. Vieren, M. Voos, and J. P. Faurie, *Phys. Rev. B* **44**, 13541 (1991).
- ¹⁹D. Calecki, J. F. Palmier, and A. Chomette, *J. Phys. C* **17**, 5017 (1984).
- ²⁰A. R. Reisinger, K. A. Harris, T. H. Myers, R. W. Yanks, L. M. Mohnkern, and C. A. Hoffman, *Appl. Phys. Lett.* **61**, 699 (1992).

Published without author corrections